Proceedings of the 11th ICPMG 2026
11th International Conference on Physical Modelling in Geotechnics
8-12 June 2026, Zurich, Switzerland

Bearing capacity of tapered piles driven in medium-dense Fontainebleau sand

L. Bałachowski
Faculty of Civil and Environmental Engineering, Gdańsk University of Technology, Gdańsk, Poland, lech.balachowski@pg.edu.pl

J. Konkol
Faculty of Civil and Environmental Engineering, Gdańsk University of Technology, Gdańsk, Poland, jakub.konkol@pg.edu.pl

L. Thorel, M. Blanc, T. Dubreucq
GERS-CG Lab, Université Gustave Eiffel, Campus de Nantes, Nantes, France, luc.thorel@univ-eiffel.fr, matthieu.blanc@univ-eiffel.fr, thierry.dubreucq@univ-eiffel.fr

ABSTRACT: Bearing capacity of tapered piles driven into medium-dense Fontainebleau sand was studied in the centrifuge tests performed at Gustave Eiffel University. Two conical models (T1, T2) with taper angle of 0.7 and 1.4 degree, respectively, and a reference straight pile (S) were installed by in-flight impact driving and then subjected to static compression tests up to the displacement of one pile diameter. The penetration depth and volume were the same for all pile models. The aim of the study was to identify the optimal pile shape with respect to installation and load-bearing capacity. It was found that the maximum head force at the end of static loading was about 15% higher for tapered models than for the cylindrical one. While the unit base resistance of tapered piles was only 15-20% larger than for the straight one, their average unit shaft friction was extremely higher than in case of cylindrical pile with almost 10 and 6 times larger value for the T2 and T1 model, respectively. By consequences, the contribution of the shaft resistance to the overall pile bearing capacity at the end of static loading makes only 4% in case of cylindrical model and up to 46% for the T2 pile. The results with impact driven installation mode were compared with previous study on monotonically installed pushed-in tapered piles.

1 INTRODUCTION

Optimizing pile geometry to achieve higher bearing capacity using the same material volume is an important topic. Various studies demonstrated the promising application of tapered piles (Kodikara and Moore, 1993; Horvath and Trochalides, 2004; Ghazavi and Kalantari, 2008; Lee et al., 2009). The model tests made by, among others, Manandhar and Yasufuku (2013), Paik et al. (2011), Shabanpour and Ghazavi (2022), and Wei and El Naggar (1998), have consistently highlighted that the tapered shape enhances shaft friction, leading to increased axial capacity of piles. The behaviours of impact driven tapered piles in sand was investigated by El Naggar and Sakr (2000), Sakr and El Naggar (2003), and Shabanpour and Ghazavi (2022) in centrifuge tests. The models were, however, installed in 1g condition, which does not permit the correct physical modelling of stress state and stress/strain changes during their penetration (El Haffar et al. 2017). The behaviour of pushed-in tapered walls in dense Fontainebleau sand using in-flight installation mode in centrifuge was studied by Bałachowski et al. (2024a). Similarly, the tapered piles pushed-in in medium-dense sand were already investigated in centrifuge tests (Bałachowski et al., 2024b). The effect of continuous installation of different shape tapered models was thus already examined for axisymmetric and plane strain conditions. This study aims to complete this investigation with in-flight impact driven tapered piles installed in medium dense sand.

2 METHODOLOGY

A wide experimental research within Geolab (2021) European project was undertaken at geotechnical centrifuge at Gustave Eiffel University (Nantes, France) in the GERS-CG lab (Gers-CG, 2023) to study the axial behaviour of tapered piles in medium-dense to dense sand during the installation, and under static axial loading. The geo-centrifuge has a radius of 5.5m, and a total mass of 2 tons can be embarked in the swinging basket with maximum acceleration level of 100g (Thorel, 2022).

2.1 Model piles

The models of piles with three different shapes: straight profile (S), 0.70 degrees (T1), and 1.4 degrees (T2) of taper angle were prepared (Figure 1). All models have almost the same volume at final embedment L=224 mm. The slenderness ratio of cylindrical pile with diameter D=16 mm is equal 14 at the end of driving. Concerning the geometrical scale of the physical models equal to 25, the prototype pile has average diameter of 400 mm and the embedment length of 5.60 m. At the base location, the models were instrumented with 5kN load cell (XF 3068) manufactured by TE Connectivity with combined error (non-linearity and hysteresis) lower than of 0,5% of the working range. Tubular piles with internal diameter of 5 mm were used (Figure 1). The axial stiffness (EA) of the cylindrical model is 13.43 MN, which corresponds to the stiffness of the prototype equal to 8391 MN.

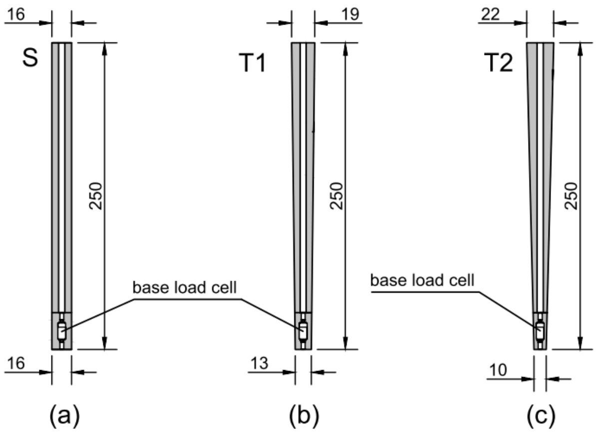

Figure 1. Model piles: (a) Straight pile, S (α=0°), (b) Tapered pile, T1 (α=0.70°), and (c) Tapered pile, T2 (α=1.4°). All dimensions are in mm.

2.2 Soil model

The strong box container with dimensions 1200 × 800 × 670 mm was filled with Fontainebleau NE 34 sand characterized by the parameters shown in Table 1. Sand-raining technique was used to prepare homogeneous soil mass with relative density of 0.56. Well calibrated automatic system with moving sand curtain was used. The designed dry bulk density of 15.52 kN/m^3 was verified with density pots after the centrifuge test. Dry sand specimen was used. Three model piles have been tested in the same strong box with at least 10 diameters inter-axes (Philips and Valsangkar, 1987; Bolton et al., 1999) (Figure 2). Each pile is considered as an isolated one. Additionally, a series of mini-CPT, 11.3 mm in diameter, was performed in the resting space of the strong box (Figure 3) to check the soil homogeneity. The test schedule is given in Table 2.

Table 1. Fontainebleau sand (NE34) parameters (Andria-Ntoanina et al., 2010; Beroya-Eitner et al., 2022).

Parameter	Property	Value	Units
Specific gravity	G_s	2.65	-
Dry density	γ_d	15.52	kN/m^3
Relative density	D_r	0.56	-
Void ratio	e_0	0.674	-
Minimum void ratio	e_{min}	0.510	-
Maximum void ratio	e_{max}	0.882	-
Effective angle of internal friction	ϕ'	34.6	°
Constant volume angle of internal friction	ϕ'_{cv}	31.5	°

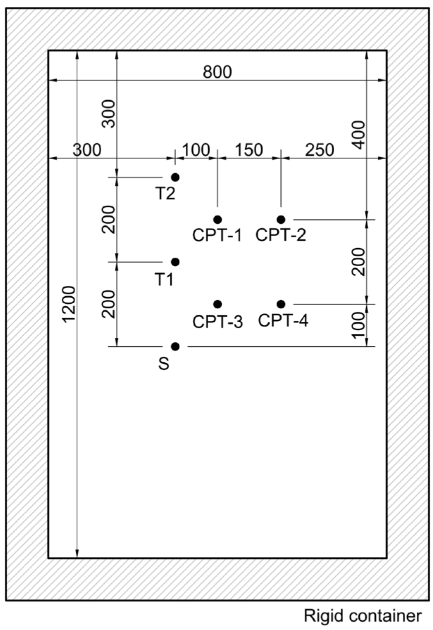

Figure 2. Strong box with position of model piles and CPT.

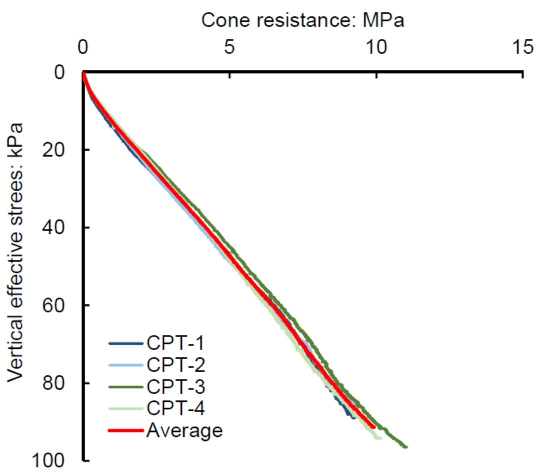

Figure 3. Cone resistance in medium dense Fontainebleau sand during centrifuge test at 25g.

Table 2. Test schedule

Item	Model test	Remarks
1	S	Pile driving and compression static loading without stopping the machine. Centrifuge stopped after the test, pile S left in place.
2	T2	Pile driving and compression static loading without stopping the machine. Centrifuge stopped after the test, pile T2 left in place.
3	T1	Pile driving and compression static loading without stopping the machine. Centrifuge stopped after the test, pile T1 left in place, loading frame with penetrometer was mounted.
4	CPT Penetrometers	CPT-1 and CPT-2 penetration tests were performed. Position of penetrometer loading frame was adjusted after stopping the centrifuge, and CPT-3 and CPT-4 were made.

2.3 Test procedure

At the beginning of each test the position of model pile was restricted within the driving guide. The steel anvil was fixed to the pile head. The pile toe penetrated 30-40 mm into the sand before spinning the centrifuge, and then its embedment progressed as the gravity increased. At operating acceleration of 25g, the pile head displacement was measured and the position of the vertical hydraulic actuator holding the hammer was controlled to maintain the required drop height. The electric fork motor was then activated and impact driving was initiated. The rotational speed of the electric motor was fixed to 30 rpm, which corresponds to one blow per second. In general, the driving energy input into the system can be adjusted according to the drop height and the mass of the ram of the hammer. In this case, the ram weighed 0.164 kg, and a drop height of 20 mm was applied. The hammer allows for the application of static compression load to the pile head after the end of driving without stopping the machine. The detailed description of the impact driving system is given in Maatouk et al. (2020, 2022) and by Weamec (2025).

Each pile was driven into the sand to the target depth of 224 mm. Afterwards, the pile was subjected to the static axial compression with a loading rate 0.1 mm/s to reach the displacement equivalent to one pile diameter (16 mm). Finally the pile head was unloaded to zero. Data acquisition of the values of head load, base load and head displacement was conducted at 0.01-second intervals.

3 EXPERIMENTAL RESULTS

3.1 Driving process

The pile embedment with number of blows is given in Figure 4. The lowest number of blows necessary to reach the target depth was observed for T1 model.

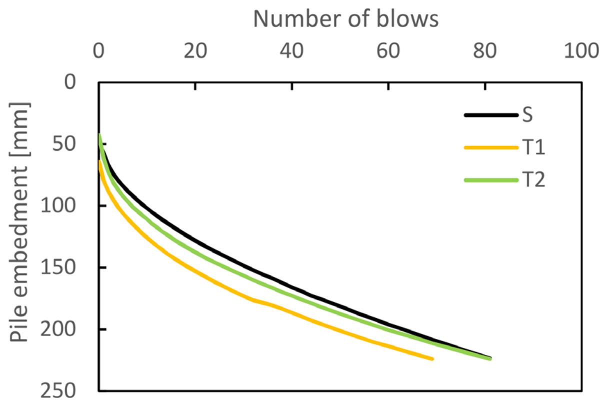

Figure 4. Model pile penetration during impact driving.

3.2 Load-settlement curves

During compression static loading the head force recorded for the cylindrical pile is slightly lower than for the conical ones. The difference increases with pile displacement and the force measured for the displacement equivalent to pile diameter (16 mm) is about 15-20% larger in case of tapered models.

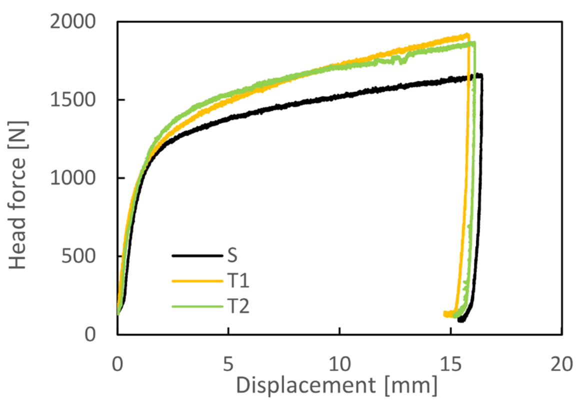

Figure 5. Head load – settlement curves during static loading test (model scale).

Table 3. Unit base resistance and average unit shaft friction

Test	Residual base resistance q_{bres} [MPa]	Ultimate base resistance $q_{b0.1D}$ [MPa]	Cone resistance q_c [MPa]	$q_{b0.1}/q_c$	Unit shaft friction $f_{c0.1D}$ [kPa]
S	0.86	5.4		0.58	4
T1	1.43	6.6	9.3	0.71	26
T2	2.48	8.3		0.89	53

3.3 Base resistance

Due to smaller base area of tapered piles the load transmitted by their toe is significantly lower than for the cylindrical one (Figure 6). Higher residual base resistance after impact driving (Figure 7) is noticed for tapered piles (see Table 3) with steeper mobilization of the unit base resistance during static loading. As a result, the unit base resistance for a given displacement level increases with taper angle. At standard failure criterion corresponding to the pile displacement s = 0.1D (where s = pile settlement), the unit base resistance for T1 and T2 is about 20% and 50% respectively higher than for straight model. The difference attenuates with displacement level.

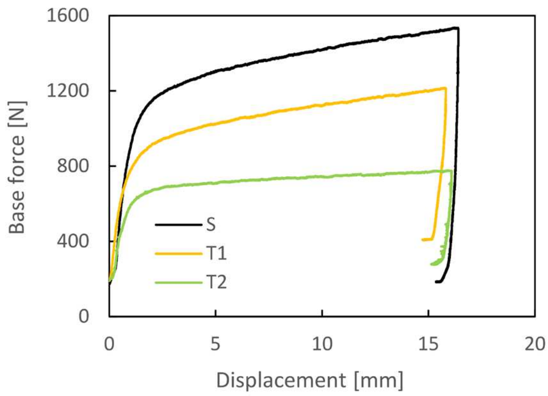

Figure 6. Base load – settlement curves during static loading test (model scale).

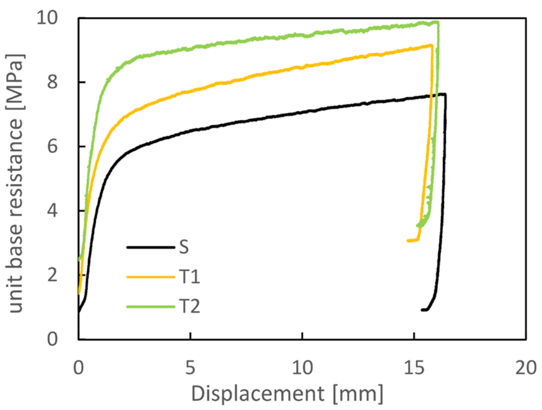

Figure 7. Mobilization of unit base resistance in static loading test (model scale).

3.4 Shaft friction

Averaged unit shaft friction mobilized during static compression test is given in Figure 8. One should notice extremely high effect of tapering (see Table 3). Shaft friction on T1 and T2 piles is respectively more than 6 and 13 times higher than for the straight model. This difference slightly attenuates with displacement level.

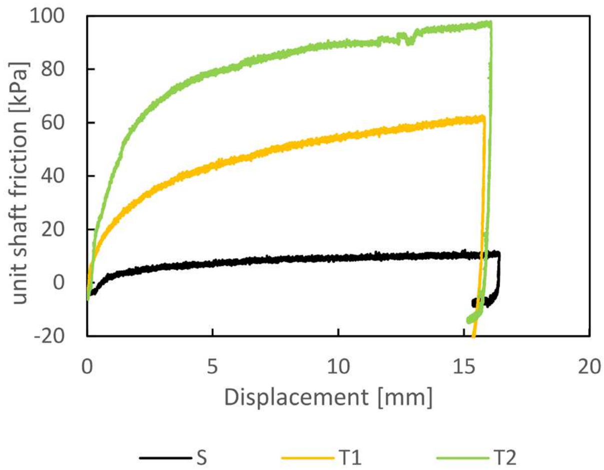

Figure 8. Mobilization of unit shaft friction during static loading test (model scale).

The average unit shaft friction can be estimated using β-method:

$$f_s = \beta \cdot \sigma'_{v0} \quad (1)$$

$$\beta = K \cdot tan(\delta_c) \quad (2)$$

where: f_s = skin friction; β = shaft friction coefficient; σ'_{v0} = initial vertical effective stress; K = lateral stress coefficient; δ_c = critical angle of interface friction.

The parameters of sand-aluminium interface were determined with interface ring shear tests at constant normal load. The surface of models is smooth with average surface roughness R_a = 0.513 µm. Taking into account the mean grain diameter of Fontainebleau NE34 sand (d_{50} = 0.21 mm) one can consider the pile-soil interface as a smooth one with relative roughness R_n = 0.0024 ($R_n = R_a/d_{50}$) smaller than the threshold value 0.01 as suggested by Garnier et al. (2007). The critical angle of interface friction estimated at normal stress 100 kPa is about 11°, which is in agreement with the interface tests performed by Lehane and White (2005). Taking into account the unit shaft friction of cylindrical pile at 1D displacement equal to 10 kPa (see Figure 8) the resulting lateral stress coefficient K in the mid-depth of the cylindrical pile (where σ'_{v0} = 44kPa) is close to 1.14. One should, however, notice that the pile surface is very smooth with contractant behaviour within interface recorded in ring shear tests. Low value of lateral stress coefficient could also result from arching developed during installation of a small diameter model. For the large diameter prototype pile with higher interface roughness such phenomena will not occur. The upscaling of the measured shaft friction on cylindrical model can not be straightforward. It should take into account the analysis of the prototype pile roughness, normal stiffness of model pile interface, advanced cyclic interface tests with constant normal stiffness and the similarity of driving process in the field conditions and centrifuge. It should also include the possible arching effect in case of small diameter model.

3.5 Driven piles versus pushed-in piles

The database concerning the bearing capacity of in-flight installed piles is still limited. The centrifuge tests (White and Lehane, 2004; d'Arezzo et al., 2013; El Haffar et al., 2017) have examined the effect of installation on pile bearing capacity. It was demonstrated (El Haffar et al., 2017) that monotonically installed piles at 100g have 8% higher bearing capacity than cyclically jacked piles. Similar effect should be expected in case of impact driven piles. The lateral stress evolution on the model pile shaft depends on the installation mode. In case of centrifuge tests the highest horizontal stationary stress was measured for pushed-in piles followed by jacked and pseudo-dynamically installed piles (White and Lehane, 2004; Lehane and White, 2005). The horizontal stationary stress for monotonically installed piles in dense sand was at a given instrument depth at least 50% higher than those recorded during cyclic installation (Gavin and Kelly, 2007). The highest shaft friction is measured on monotonically installed piles with cyclic shear degradation observed for jacked and driven piles.

Tapered piles are characterized by high contribution of the shaft to overall pile bearing capacity (Figure 9). While it makes only about 4% for cylindrical model, this contribution constitutes up to 25% and 46% in case of T1 and T2 pile, respectively, in case of standard failure criterion s = 0.1D. The previous tests on pushed-in model piles (Bałachowski et al., 2025b) indicate slightly higher values (Figure 9). The contribution of shaft resistance to overall capacity of pushed-in piles is similar to the value of 8% observed (d'Arezzo et al., 2013) for in-flight continuous penetration in a very dense sand. In case of cyclic installation with strokes they noticed the reduction of shaft resistance due to cyclic degradation of interface shear strength. Similar effect was also observed in centrifuge tests by White and Lehane (2004), and Lehane and White (2005). For the impact driven cylindrical pile in this study such small contribution of shaft resistance to overall bearing capacity seems, however, too low.

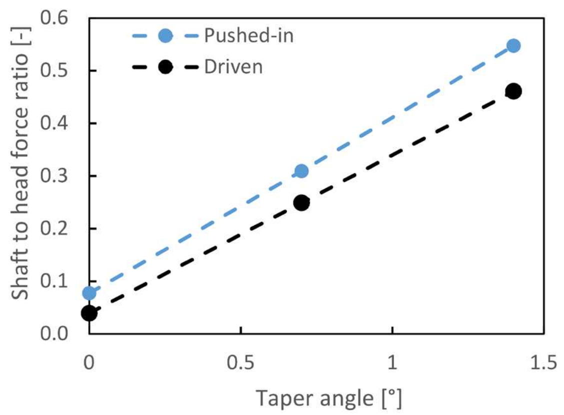

Figure 9. Shaft contribution to overall pile bearing capacity.

The mobilization of average shaft friction for pushed-in and driven piles (Bałachowski et al, 2024b) in medium dense sand is compared in Figure 10. One can notice steeper friction mobilization in case of piles installed by continuous pushing. At large displacement equal to 1D, the shaft friction developed for pushed-in models is more than 20% higher than for impact driven installation. Very similar behaviour is observed for unit base resistance (Figure 11). Pushed-in piles are characterized by very sharp increase of resistance, while the mobilization for driven piles is much smoother. The unit base resistance mobilized at 1D is also about 20% higher for pushed-in piles than for impact driven piles. In order to explain such difference one should consider the driving process. The base rebound after each impact together with the consecutive cyclic loading of the soil in the vicinity of the pile base could be the reason of softer response of the base of driven pile compared to the pushed-in one. The base rebound was not measured. At the end of pile driving the rebound of pile head was about 0.1mm (2.5mm in the prototype scale) which is not excessive value. Due to a single impact the stress applied to the base varried from 0.4 to 1.2 MPa, which is much lower than the base resistance during continuous pile penetration. This could also lead to lower radial stress mobilized due to pile driving than in continuous penetration.

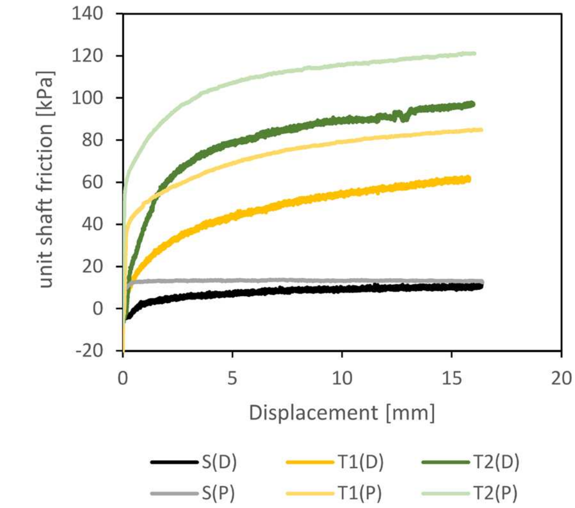

Figure 10. Unit shaft friction for driven and pushed-in installation. Note: D and P in brackets indicate driven and pushed-in piles, respectively.

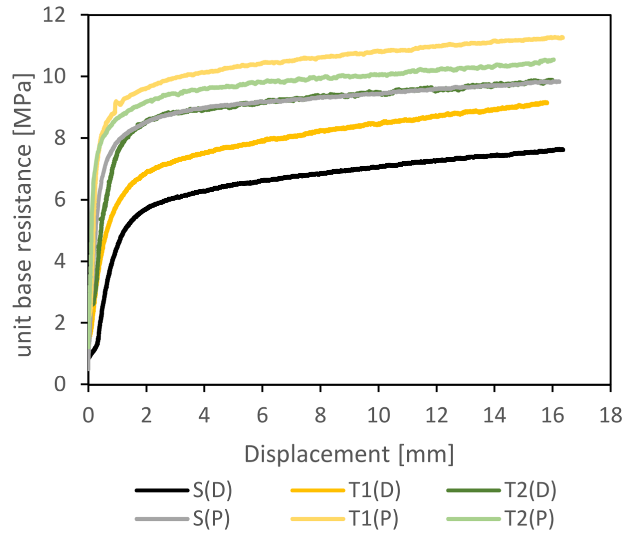

Figure 11. Unit base resistance for driven and pushed-in installation. Note: D and P in brackets indicate driven and pushed-in piles, respectively.

4 CONCLUSIONS

The presented tests confirmed the high contribution of shaft resistance to overall capacity of impact driven tapered piles, which significantly increases with taper angle. For the pile head displacement of 0.1D the friction force constitutes only approx. 4% of total load in case of cylindrical pile, but it makes up to 25% and 46% for T1 and T2, respectively. This contribution is slightly lower than observed for pushed-in models. The study confirms high impact of tapering on shaft friction. High shaft friction on tapered piles compensates lower contribution of the force transmitted by their smaller base. For standard failure criterion the head force for tapered models is slightly higher than for cylindrical one. The difference increases to about 15% at the end of static load, i.e. for the displacement equal to one pile diameter. This study confirms higher efficiency of impact driven tapered piles over the cylindrical one. Different schemes of shaft friction development were observed for driven and pushed-in models with steep mobilization for the latter. For large displacement the shaft friction in case of continuous pushing was considerably higher than for impact driven piles. Similarly, the unit base resistance derived for pushed-in models was more than 20% higher than in case of impact driven piles. The study confirms high impact of installation mode on bearing capacity of model piles. The normal stress increase imposed during tapered pile penetration is the principal mechanism to explain high impact of tapering on shaft resistance. The existing database concerning bearing capacity of in-flight installed piles is still limited. The construction and use of new pile driving systems will be very advantageous for better understanding the impact of the installation mode on pile bearing capacity.

ACKNOWLEDGEMENTS

This project has received funding from the European Union’s Horizon 2020 research and innovation program under Grant Agreement No. 101006512. The Geolab project is greatly acknowledged.

REFERENCES

Andria-Ntoanina, I., Canou, J. and Dupla, J.C. (2010). *Caractérisation mécanique du sable de Fontainebleau NE34 à l’appareil triaxial sous cisaillement monotone.* Laboratoire Navier–Géotechnique: CERMES, ENPC/LCPC.

Bałachowski L., Kabeta, W.F., Thorel, L., Blanc, M. and Dubreucq T. (2024a). Centrifuge modelling of tapered wall jacked into medium dense sand. In: *Proceedings of the XVIII European Conference on Soil Mechanics and Geotechnical Engineering,* N. Guerra, C. Ferreira, A.G. Correia and M.M. Fernandes (eds.), ISSMGE, Lisbon, Portugal, pp. 1–4. https://doi.org/10.1201/9781003431749-35

Bałachowski, L., Kabeta, W.F., Konkol, J., Thorel, L., Blanc, M. and Dubreucq, T. (2024b). Bearing capacity of monotonically installed tapered piles in medium-dense Fontainebleau sand. In: *Proceedings of the 5th European Conference on Physical modelling in Geotechnics*, M.A. Cabrera et al. (eds.), ISSMGE, Delft, The Netherlands, pp. 1-6. https://doi.org/10.53243/ECPMG2024-74

Beroya-Eitner, M.A., Machaček, J., Viggiani G, et al. (2022). GEOLAB Material Properties Database. https://doi.org/10.5281/zenodo.7462287

Bolton, M.D., Gui, M.W., Garnier, J., et al. (1999). Centrifuge cone penetration test in sand. Geotechnique, 49(4), 543-552. https://doi.org/10.1680/geot.1999.49.4.543

d'Arezzo, B.F., Haigh, S. and Ishihara Y. (2013). Cyclic jacking of piles in silt and sand. In: *Installation Effects in Geotechnical Engineering*, M.A. Hicks et al. (eds.), CRC Press, Rotterdam, The Netherlands, pp. 86–91.

El Haffar I., Blanc M., Thorel L. (2017). Impact of pile installation method on the axial capacity in sand. *Géotechnique Letters*, 7(3): 260-265. http://dx.doi.org/10.1680/jgele.17.00036

El Naggar, M.H.E. and Sakr, M. (2000). Evaluation of axial performance of tapered piles from centrifuge tests. *Canadian Geotechnical Journal,* 37(6): 1295–1308. https://doi.org/10.1139/t00-049

Garnier, J., Gaudin, C. and Springman, S.M., et al. (2007). Catalogue of scaling laws and similitude questions in geotechnical centrifuge modelling. *International Journal of Physical Modelling in Geotechnics,* 7(3): 01–23. https://doi.org/10.1680/ijpmg.2007.070301

Gavin, K.G. and O'Kelly, B.C. (2007). Effect of friction fatigue on pile capacity in dense sand. *Journal of Geotechnical and Geoenvironmental Engineering,* 133(1): 63-71. https://doi.org/10.1061/(ASCE)1090-0241(2007)133:1(63)

Geolab (2021). Geolab – Science for enhancing Europe's Critical Infrastructure. https://project-geolab.eu/

Gers-CG (2023). Centrif-UGE. https://cg.univ-gustave-eiffel.fr/2/centrif-uge

Ghazavi, M. and Kalantari, A.B. (2008). Experimental Study of Taper Piles With Different Taper Angles. In: *Proceedings of the 27th International Conference on Offshore Mechanics and Arctic Engineering, Volume 2: Structures, Safety and Reliability*, Estoril, Portugal, pp. 65–69. https://doi.org/10.1115/OMAE2008-57110

Horvath, J.S. and Trochalides, T. (2004). A half century of tapered-pile usage at the John F. Kennedy International Airport. In: *Proceedings of 5th International Conference on Case Histories in Geotechnical Engineering*. University of Missouri–Rolla, New York, USA, pp. 11.05

Kodikara, J. K. and Moore, I. D. (1993). Axial response of tapered piles in cohesive frictional ground. *Journal of Geotechnical Engineering*, 119(4): 675-693. https://doi.org/10.1061/(ASCE)0733-9410(1993)119:4(675)

Lee, J., Paik, K., Kim, D. and Hwang, S. (2009) Estimation of Axial Load Capacity for Bored Tapered Piles Using CPT Results in Sand. *Journal of Geotechnical and Geoenvironmental Engineering*, 135(9): 1285–1294. https://doi.org/10.1061/(ASCE)GT.1943-5606.0000036

Lehane, B.M. and White, D.J. (2005). Lateral stress changes and shaft friction for model displacement piles in sand. *Canadian Geotechnical Journal,* 42(4): 1039-1052. https://doi.org/10.1139/t05-023

Maatouk, S., Blanc, M. and Thorel, L. (2020). Development of a Hammer to drive monopiles of offshore wind turbines in Centrifuge. In: *Proceedings of the 4th European Conference on Physical Modelling in Geotechnics,* J. Laue and T. Bansal (eds.), ISSMGE, Luleå, Sweden, pp. 89-93.

Maatouk, S., Blanc, M., & Thorel, L. (2022). Impact driving of monopiles in centrifuge: effect on the lateral response in sand. *International Journal of Physical Modelling in Geotechnics*, 22(6): 318-331. https://doi.org/10.1680/jphmg.21.00035

Manandhar, S. and Yasufuku, N. (2013). Vertical bearing capacity of tapered piles in sands using cavity expansion theory. *Soils and Foundations*, 53(6): 853-867. https://doi.org/10.1016/j.sandf.2013.10.005

Paik, K., Lee, J. and Kim, D. (2011). Axial Response and Bearing Capacity of Tapered Piles in Sandy Soil. *Geotechnical Testing Journal*, 34(2): 102761. https://doi.org/10.1520/GTJ102761

Phillips, R. and Valsangkar, A. (1987). An experimental investigation of factors affecting penetration resistance in granular soils in centrifuge modelling, Technical report: CUED/DTR210.

Sakr, M. and El Naggar, M.H. (2003). Centrifuge Modeling of Tapered Piles in Sand. *Geotechnical Testing Journal*, 26(1): 22-35. https://doi.org/10.1520/GTJ11106J

Shabanpour, A. and Ghazavi, M. (2022). Centrifuge tests on axially loaded tapered piles with different cross-sections under compressive and tensile loading. *Canadian Geotechnical Journal*, 59(7): 1205–1214. https://doi.org/10.1139/cgj-2020-0732

Thorel, L. (2022). Physical Modelling Facilities: from Galileo to 3D Printing. In: *10th ICPMG Int. Conf. on Physical Modelling in Geotechnics*. Korean Geotechnical Society (KGS), Daejon, Korea, pp. 64–72.

Weamec (2025). Weamec: a multidisciplinary network dedicated to marine renewable energy https://www.weamec.fr/en/technologies/pile-driver-for-centrifuge-models/

Wei, J. and El Naggar, M.H. (1998). Experimental study of axial behaviour of tapered piles. *Canadian Geotechnical Journal*, 35(4): 641–654. https://doi.org/10.1139/t98-033

White, D.J., and Lehane, B.M. (2004). Friction fatigue on displacement piles in sand. *Géotechnique*, 54(10): 645–658. https://doi.org/10.1680/geot.2004.54.10.645.